Chiral Aggregation Phenomena. 3. Chiral Discrimination in the Monolayer Packing of N-(α-Methylbenzyl)stearamides on Aqueous Acid Subphases: Thermodynamic Behavior

Edward M. Arnett,* Jean Chao, Barbara J. Kinzig, Martin V. Stewart, Orlean Thompson, and Robert J. Verbiar

Contribution from the Departments of Chemistry, Duke University, Durham, North Carolina 27706, and University of Pittsburgh, Pittsburgh, Pennsylvania 15260.
Received July 23, 1981

Abstract: The study of monolayers at the air–liquid interface offers unusual opportunities to investigate the effects of stereochemical factors in organized systems. As a first step toward developing this field, we have examined some surface properties of N-(α-methylbenzyl)stearamide, comparing the behavior of monolayer films of its racemic modification with its two enantiomeric forms and also with the achiral position isomer N-phenethylstearamide. X-ray powder diffraction patterns showed that the racemic material was, in fact, a true racemate. Also, the transition points and heat of fusion of the racemate were markedly different from those of the enantiomers, as shown by differential scanning calorimetry. Although the stearamides did not spread as monolayers on water as a subphase, aqueous sulfuric acid media above 6 N evoked good surfactant behavior as manifested by reduction of the subphase surface tension. Chiral discrimination was clearly apparent in the monolayer behavior and was sharply acid dependent. Thus, the racemic N-(α-methylbenzyl)stearamide began to show surface activity on 6 N H_2SO_4 while the enantiomers required 8 N acid to give the same response. Equilibrium spreading pressures (ESP's) for the films in equilibrium with the pure crystals were measured on a Langmuir film balance as a function of subphase acidity and temperature. Thermodynamic properties for the surface films were evaluated from these ESP values and also from static surface tension measurements made at different temperatures. By all criteria, the molecules of the optically pure samples are more strongly and completely associated, both in the crystalline and in the monolayer phase, than are those of the racemate. We propose that the acid dependence of chiral discrimination between enantiomeric and racemic films is caused by protonation of the amide head group by the aqueous acid subphase. This produces a driving force for expansion of the film which is opposed by the aggregation forces in the neutral amide molecules. These forces are stronger for the enantiomers than for the racemate. As a test of this model, a series of liquid–liquid distribution experiments was performed for the transfer of N-(α-methylbenzyl)butyramide from hexane to the series of aqueous acid solutions used for monolayer subphases. A close correlation was found between the acid dependence of the free energy of spreading for the stearamide and the free energy of transfer of the butyramide. The pK_{BH^+} of the butyramide was calculated to be -1.5 ± 0.5 from the distribution experiments and -1.5 ± 0.2 from an independent series of indicator measurements. The free energy correlation suggests that the pK_{BH^+} of the protonated stearamide at the air–acid interface is close to that of the butyramide in homogeneous solution. The force-area behavior and dynamic properties of the monolayers will be reported subsequently. This paper is limited to a description of the thermodynamic properties under bona fide reversible conditions.

Introduction

The aggregation of molecules and ions plays an important role in most chemical reactions in condensed phases. The past decade has seen enormous progress in our ability to differentiate inherent contributions (i.e., those observed in the gas phase) to structure-reactivity patterns from factors which are produced by interactions in condensed environments.[1-10] It is convenient to catalog a variety of types of relatively weak intermolecular and interionic forces (e.g., London dispersion forces, ion-dipole forces, hydrogen bonding, etc.[11-13]) as "solvation forces". However, the detailed modeling of solute–solvent interactions is an enormously complex statistical problem in three dimensions because the way that the molecular and ionic units fit together is affected by their sizes and shapes as well as by the blend of forces between partners or aggregates. As a result, more progress has come from phenomenological[14-17] than from purely theoretical approaches.

In the hope of simplifying, or at least identifying, some of the important factors which influence the ways that molecules and ions fit together in condensed systems, we have chosen to apply the powerful *absolute* tool of stereochemistry to several types of systems where aggregation is defined clearly and unambiguously (e.g., in ion pairs[18] and in monolayers at the air–water interface).[19-21]

Enantiomers are perfect physical and chemical models for each other since all of their properties are identical except those which involve their interaction with other chiral systems. It is, therefore, always possible (although admittedly very time consuming) to check the accuracy of a given measurement on a chiral molecule, ion, or aggregate by comparing it with the same measurement on its enantiomer. Unless the two agree within the desired level of precision, some unknown factor such as an impurity is intro-

* To whom correspondence should be addressed at Duke University.

(1) Arnett, E. M. *Acc. Chem. Res.* **1973**, *6*, 404. Arnett, E. M.; Chawla, B. *J. Am. Chem. Soc.* **1979**, *101*, 7141.
(2) Brauman, J. I.; Blair, L. K. *J. Am. Chem. Soc.* **1970**, *92*, 5986.
(3) Olmstead, W. N.; Brauman, J. I. *J. Am. Chem. Soc.* **1977**, *99*, 4219.
(4) Taft, R. W. "Proton-Transfer Reactions"; Caldin, E. F.; Gold, V., Eds.; Chapman and Hall: London, **1975**. Taft, R. W.; Wolf, J. F.; Beauchamp, J. L.; Scorrano, G.; Arnett, E. M. *J. Am. Chem. Soc.* **1978**, *100*, 1240.
(5) Taagepera, M.; De Frees, D.; Hehre, W. J.; Taft, R. W. *J. Am. Chem. Soc.* **1980**, *102*, 424 and articles cited therein.
(6) Beauchamp, J. L. *Annu. Rev. Phys. Chem.* **1971**, *22*, 527.
(7) MacKay, G. I.; Hemsworth, R. S.; Bohme, D. K. *Can. J. Chem.* **1976**, *54*, 1624.
(8) Kebarle, P. *Annu. Rev. Phys. Chem.* **1977**, *28*, 445.
(9) Lias, S. G.; Ausloos, P. "Ion-Molecule Reactions"; American Chemical Society: Washington, DC, 1975.
(10) Bowers, M. T., Ed. "Gas Phase Ion Chemistry"; Academic Press: New York, 1979.
(11) Jencks, W. P. "Catalysis in Chemistry and Enzymology"; McGraw-Hill: New York, 1969.
(12) Kauzmann, W. *Adv. Protein Chem.* **1959**, *14*, 1.
(13) Tanford, C. "The Hydrophobic Effect", 2nd ed.; Wiley: New York, 1980.
(14) Reichardt, C. "Solvent Effects in Organic Chemistry"; Verlag Chemie: New York, 1979.
(15) Koppel, I. A.; Palm, V. A. In "Advances in Linear Free Energy Relationships"; Chapmen, N. B., Shorter, J., Eds.; Plenum Press: New York, 1972.
(16) Kamlet, M. J.; Abboud, J. L. M.; Taft, R. W. *Prog. Phys. Org. Chem.* **1980**, *13*, 485.
(17) Amis, E. S.; Hinton, J. F. "Solvent Effects on Chemical Phenomena"; Academic Press: New York, 1973.
(18) Arnett, E. M.; Zingg, S. P. *J. Am. Chem. Soc.* **1981**, *103*, 1221.
(19) Arnett, E. M.; Chao, J.; Kinzig, B.; Stewart, M.; Thompson, O. *J. Am. Chem. Soc.* **1978**, 100, 5575.

0002-7863/82/1504-0389$01.25/0

ducing an error into one or both measurements. Conversely, the observation of different behavior for a racemic modification obtained by mixing these enantiomers together establishes a rigorous relationship between the geometrical requirements of molecular packing and the strength of the intermolecular forces by which the system aggregates. This type of comparison is *absolute* in the sense that it depends on the symmetry properties of the models under examination rather than on the usual indirect tests for consistency using molecular analogies, linear free energy extrapolations, or theoretical models. Since intermolecular forces are mostly rather weak and are often poorly defined geometrically, such an absolute check is of particular value.

The attraction of the monolayer state for the study of intermolecular forces lies in the fact that there is a much higher degree of orientation of surfactant molecules at the air–water interface than is found in the usual three dimensions in solution. Furthermore, there is an unparalleled opportunity for the experimenter *to control the orientation* of the molecules at the interface by varying the surface area per molecule.

The techniques for spreading, transferring, and studying monolayers at the air–water interface have been described in a number of excellent monographs[22-29] which outline the development of the field since its beginning in the laboratories of Pockels[30] and of Langmuir and Blodgett.[31] In recent years biophysicists have been particularly active in the study of lipid monolayers as more or less simplified models for bilayer cell membranes.[32]

Despite the fact that most of the components of biomembranes are chiral (as also are many of the biologically important molecules which traverse them) only a handful of experimental studies have been aimed deliberately at examining the role of intermolecular stereochemistry in the packing of chiral surfactants in monolayers.[33] The purpose of the present work is to combine the powerful principles of stereochemistry with the elegant techniques of monolayer manipulation in order to elucidate the contribution that molecular shape may make to aggregation in oriented systems.

To gain an entree to the field of chiral monolayers, we chose to take advantage of the well-established stereochemical properties of (α-methylbenzyl)amine with the thoroughly investigated monolayer behavior of stearic acid and its derivatives. Accordingly, the amine and stearoyl components were joined to make both enantiomers of the amide (*R*)-(+)- and (*S*)-(−)-*N*-(α-methylbenzyl)stearamide, whose absolute configuration was thereby established from that of the precursor amine.

This paper, and following ones, will describe our studies with monolayers of these enantiomeric amides and their racemate on a series of aqueous sulfuric acid subphase solutions. Some comparisons will also be made with the behavior of the achiral position isomer, the stearamide of 2-phenylethylamine.[34]

Acid subphases were employed when we found that strong aggregation forces in the neutral stearamides prevented spreading to produce a monolayer. These media ionized the amide head group and caused expansion of the film to produce a monolayer. Furthermore, clear chiral discrimination between the properties of films cast from the enantiomeric amides and those from the racemate established that this system could be used to examine the effects of stereochemistry on molecular packing in monolayers. The acid dependence of the chiral discrimination behavior *is a previously unpublished phenomenon in monolayer chemistry*[35] with possible implications for the pH dependence of chiral interactions in biomembranes.

In this paper, we will describe those properties of the chiral amide monolayers which are probably truly thermodynamic and also the experimental equipment and methodologies used in our laboratory. In view of the well-known difficulties of monolayer research and the somewhat subtle effects we wished to study, the experimental work will be described in detail. Subsequent reports will describe chiral discrimination in the time-dependent (dynamic) behavior of the films and a further interpretation of the experimental results.

Experimental Section

General Chemical and Instrumental Methods. Monolayers are notoriously sensitive to contamination. At every point in the synthesis, purification, storage, solution preparation, and actual film-balance experiments, there is risk of contaminating samples with film-forming impurities which could lead eventually to mixed monolayers of complex composition whose surface properties might differ greatly from those of the pure surfactant under study. Lipid material can be introduced from the hands of the experimentalist, from residual grease in glassware, from soap, cosmetics, and tobacco smoke, and from oily particles dispersed as aerosols from vacuum pumps and motors.[36,37] Accordingly, all of the routine chemical manipulations of an ordinary synthetic laboratory were conducted under conditions of cleanliness comparable to those finally used in the film-balance laboratory itself. Fortunately, the absolute method of comparing enantiomers, as described in the introduction, can be applied as an important check on the ultimate purity of the final surfactant products during the actual film-balance experiments.

All equipment such as ovens which might have oil contamination were purchased new for the project and dedicated to it. Likewise, all glassware was new and dedicated so that it never contacted grease of any kind. It was handled either with nichrome tongs or plastic gloves that were shown to be free of transferable plasticizers. All chemical samples were isolated from oil pumps by activated carbon cartridges and acetone–Dry Ice traps. Suction filtration funnels were covered to filter out airborne contamination. Reactions and distillations were conducted under nitrogen which passed through activated charcoal (8–12 mesh), concentrated sulfuric acid, and sodium hydroxide pellets. Careful attention was paid to all construction materials which contacted the samples. All glassware (except for calibrated volumetric vessels) was soaked successively in solutions of ethanolic KOH (120 g KOH in a mixture of 120 mL of water/L of 95% ethanol), HNO_3–H_2SO_4 (1:2, 130 °C), and pure water and then stored in a clean oven at 150 °C until needed. This latter precaution was necessary to minimize the condensation or adsorption of film-forming organic materials from the laboratory air.[36] Laboratory grease was

(20) Arnett, E. M.; Thompson, O. *J. Am. Chem. Soc.* **1981**, *103*, 968.
(21) Stewart, M. V.; Arnett, E. M. *Top. Stereochem.* in press.
(22) Gaines, G. L. "Insoluble Monolayers at Liquid-Gas Interfaces"; Interscience: New York, 1966.
(23) Adam, N. K. "The Physics and Chemistry of Surfaces", 3rd ed.; Oxford University Press: London, 1941.
(24) Harkins, W. D. "The Physical Chemistry of Surface Films"; Reinhold: New York, 1952.
(25) Adamson, A. W. "Physical Chemistry of Surfaces", 3rd ed.; Wiley-Interscience: New York, 1976.
(26) Davies, J. T.; Rideal, E. K. "Interfacial Phenomena", 2nd ed.; Academic Press: New York, 1963.
(27) Goddard, E. D., Ed. *Adv. Chem. Ser.* **1975**, *No. 144*.
(28) Stenhagen, E. In "Determination of Organic Structures by Physical Methods"; Braude, E. A., Nachod, F. C., Eds.; Academic Press: New York, 1955; Chapter 8.
(29) Gershfeld, N. L. *Annu. Rev. Phys. Chem.* **1976**, *27*, 349. This is an excellent recent review of the field and subjects some commonly held assumptions to close scrutiny.
(30) Pockels, A. *Nature (London)* **1891**, *43*, 437.
(31) Langmuir, I. *J. Am. Chem. Soc.* **1917**, *39*, 1848.
(32) Cadenhead, D. A. In "Chemistry and Physics of Interfaces, II"; Ross, S., Ed.; American Chemical Society: Washington, DC, 1971; p 28.
(33) We have reviewed the present status of chiral monolayers in ref 21. The related field of chiral surfactants in micellar systems is currently quite active in the search for stereospecific biomimetic systems as enzyme models. Although the micellar state involves some of the same interesting factors which make monolayer study appealing, there is no means for directly controlling the orientation of molecules in micelles as there is in monolayers.
(34) This compound is often referred to as β-phenethylamine and α-(methylbenzyl)amine as α-phenethylamine. Throughout this paper we shall reserve the term phenethylamine for the achiral isomer.
(35) See, however, the thesis of F. J. Zeelen, University of Leiden, 1956. We are grateful to Dr. Zeelen for calling this work to our attention.
(36) Mysels, K. J.; Florence, A. T. In "Clean Surfaces"; Goldfinger, G., Ed.; Marcel Dekker: New York, 1973. Although most authors of monolayer articles are aware of the general problem of contamination, few of the published accounts in the field describe a thorough and routine effort to detect or prevent all of the principal known sources. This is doubtless one reason for discrepancies in published data. In the present case, the stereochemical check of the surface properties of one enantiomer against another provides considerable protection against artifacts due to impurities.
(37) See the doctoral thesis of Orlean Thompson, Department of Chemistry, University of Pittsburgh, 1980, for a detailed discussion.
(38) O'Connor, R. T.; Allen, R. R.; Chipault, J. R.; Herb, S. F.; Hoerr, C. W. *J. Am. Oil Chem. Soc.* **1966**, *43*, 10A.
(39) Rogozinski, M. *J. Gas Chromatogr.* **1964**, *2*, 328.
(40) For reviews see: Sheppard, A. J.; Iverson, J. L. *J. Chromatogr. Sci.* **1975**, *13*, 448. Christie, W. W. *Top. Lipid Chem.* **1973**, *3*, 171. Ackman, R. G. *Prog. Chem. Fat Other Lipids* **1972**, *12*, 165.

avoided through the use of Teflon stopcocks and Teflon sleeves for standard-taper joints. Aluminum foil, used to cover flasks and beakers, was rinsed with 95% ethanol to remove machining oil and then rinsed with pure water and stored at 150 °C until needed.

Reagent grade materials were employed for ordinary chemical work, and spectral grade solvents were used for spectroscopic analysis and optical rotation measurements, without further purification than is specifically described. ACS reagent grade petroleum ether (30–60 °C) and chloroform, employed for solvent extraction, were stirred for several hours over aluminum oxide (Woelm basic, activity grade I) and gravity filtered immediately prior to use. Likewise, the water employed in all solvent extractions and chemical reactions was triply distilled water from the surface laboratory.

Melting points were recorded in oven-dried, open glass capillaries using a Thomas-Hoover oil-immersion apparatus and were corrected through an in situ thermometer calibration involving seven fixed temperatures. Boiling points, however, were uncorrected. Elemental analyses were performed by Galbraith Laboratories. The densities of liquids were obtained in units of g/cm^3 by weighing the fluid in a 2-mL Gay-Lussac type specific gravity bottle calibrated to 2.1004 ± 0.0018 cm^3.

Most solutions for analytical work were prepared in volumetric flasks calibrated through measurements of the apparent density of triply distilled water. The precision of the calibrated volumes averaged near ±0.1% up to 10 cm^3 and less than ±0.1% for larger volumes. When uncalibrated glassware was employed, volumetric uncertainties were approximated by the manufacturer's specification of accuracy. Buoyancy of air corrections were applied both during the glassware calibrations and density measurements.[41] The precision of all derived quantities were computed through indeterminate error analysis using the variances estimated from all instrumental, volumetric, and gravimetric uncertainties.

Optical rotations were measured with a Perkin-Elmer 241 polarimeter with accuracy of observed rotations, α_λ^t, being ±0.002° for rotations of the plane of polarization under 1° and ±0.2% for rotations over 1°. The optical null point was established by a solvent blank prior to the measurement of each sample. Perkin-Elmer no. 017047 micropolarimeter cells having a 1-dm path length and optical glass faces (transmitting radiation to ca. 320 nm) were employed. The lengths of these cells were calibrated by the manufactuer to ±0.0001 dm. Samples were thermostated (±0.1 °C) by circulating water from a Thermomix 1480 (B. Braun Instruments) temperature controller through the jacketed polarimeter cell. Final dilution of the solutions was accomplished with the volumetric flask immersed in the circulating water bath set to the temperature of the measurement. Solution concentrations reported for specific rotations and ^{1}H NMR spectra were expressed as g/100 cm^3 of solution. Optical purity was defined empirically as the ratio of the measured specific rotation to its maximum value, $p = 100([\alpha^t_D/[\alpha^t_{D,max}])$, for a given temperature, solvent, and sample concentration.[42]

^{1}H NMR spectra[43] were recorded in ppm (δ), with 2% tetramethylsilane as an internal standard. Routine spectra (60 MHz) were obtained at ambient instrument temperature from either a Varian Associates A-60D or EM-360 NMR spectrometer and were uncalibrated. The spectra of the stearamides were recorded specially by Mr. Robert Bittner at 250 MHz using an instrument built at Mellon Institute and handled through the Mellon-Pitt Carnegie Corp. The following letters denote multiplicity: s, singlet; t, triplet; q, quartet; and m, muliplet.

Ultraviolet spectra were recorded against the appropriate reference on a Cary Model 15 spectrophotometer using matched 1.000-cm cells (Fisherbrand Suprasil QS282, path length ±0.5%). The absorbance was measured from a base line obtained by scanning an identical system without the sample.

Gas–liquid partition chromatography, GLPC, was conducted isothermally on a Hewlett-Packard 5700A gas chromatograph equipped with dual thermal conductivity detectors and heated injector ports having glass liners. Helium of 99.995% purity (High Purity, Air Products and Chemicals, Inc.) was passed through a 5A molecular sieve drier and a Supelco carrier gas purifier for use as carrier phase. Quantification of the results was assisted by a Hewlett-Packard 3380S integrating recorder; however, trace analysis was accomplished by hand through triangulation of the peak areas from a second simultaneously operated strip chart recorder.

Purification and Analysis of Stearic Acid and Methyl Stearate (Including a Note of Caution Regarding "High Purity" Commercial Samples). Special attention was given to the selection, purification, and analysis of the initial stearic acid source. The standard analytical method for fatty acids involved GLPC examination of their methyl esters,[38–40] the synthetic precursors of the stearamides. The methanolysis product of an advertised "high purity" (99.5%) stearic acid sample, mp 67.1–68.3 °C (corrected), sold by a well-respected supplier exhibited at least *13 well-resolved peaks in addition to methyl stearate on GLPC analysis.* Clearly, this was unacceptable for our purposes, and it was too expensive to warrant further purification in our laboratory. Similar analyses were made of several other commerical samples having intermediate purity. We note that stearic acid is often used as a primary standard in monolayer research. Unless its purity is confirmed rigorously before use, it may be a source of contamination or error.

Our final choice of supplier was based on the absence of branched-chain and unsaturated fatty acids in the unpurified sample, because the stearamide derivatives from the subsequent aminolysis reaction are insufficiently volatile to analyze for homologues and other such germane impurities by GLPC.

Stearic acid obtained from United States Biochemical Corp. (catalog no. 21830, 95%+), mp 66.2–68.3 °C (corrected), was purified through four to five recrystallizations either from acetone or 95% ethanol, followed by three to four recrystallizations from benzene to afford 10–20% of the original sample as white platelets, mp 69.0–69.4 °C (corrected) (lit[44] 69.6 °C). Only saturated, straight-chain fatty acids were detected in the original commercial stearic acid sample. The major constituents were found to be lauric (0.5 mol %), myristic (0.6 mol %), palmitic (3.3 mol %), and stearic (95.6 mol %) acids; however, peaks corresponding to trace amounts of all odd and even homologues from C_{10} to C_{20} were observed. Samples recrystallized seven to nine times ranged from 99.6 to 99.9 mol % pure stearic acid with only trace amounts of the C_{16}–C_{20} homolgues present.

Analysis of the methyl esters[38–41] was accomplished by GLPC using a 12 ft by $^1/_8$ in. stainless steel column packed with 20% DEGS on Chromosorb WAW (80/100 mesh) operated isothermally at 180 °C with TC detector at 250 °C (filament current 223 mA), heated injector port at 200 °C, 60 psi head pressure of He carrier gas, and a flow rate between 50 and 60 mL/min. Relative integrations obtained as area % were converted to mole % through use of the relative response factors of Killheffer and Jungermann.[45,46] After injecting samples spiked with several authentic methyl ester standards, we plotted the data as log retention time vs. carbon numbers.[47,48] Homologous fatty acid methyl esters were identified easily from the resulting linear correlation.

The resolution and sensitivity of these analytical methods for detecting potential impurities were tested through the quantitative saponification and methanolysis of a sample of ordinary beef tallow[38]. Analysis of the crude product and also a quantitatively hydrogenated sample (0.3 g of crude methanolysis product stirred magnetically over 0.3 g of 10% Pd-on-C in 20 mL of anhydrous methanol for 2 h under a hydrogen atmosphere at room temperature) demonstrated our ability to detect trace amounts of branched and unsaturated fatty acids and many unidentified components in the presence of the saturated, straight-chain homologues.

Methyl stearate was prepared for synthetic purposes by gently refluxing 20.0 g (70.3 mmol) of stearic acid in 595 mL of anhydrous methanol and 5.2 mL of concentrated sulfuric acid with magnetic stirring for 3 h.[38] The colorless solution was cooled to room temperature, diluted with 900 mL of triply distilled water, and then extracted twice against 500-mL portions of petroleum ether. The combined organic phase was extracted seven to twelve times against 200-mL portions of water until the washings were found neutral to methyl red and then dried overnight with anhydrous sodium sulfate. Gravity filtration and rotary evaporation of the solvent under reduced pressure (with continued heating of the melt for several hours over a hot-water bath) afforded consistently a 93–99% crude yield of white, impacted crystals having a melting point of 38.3–39.2 °C (corrected) (lit.[49] 38.8 °C): ^{1}H NMR (20%, $CDCl_3$, 60 MHz) δ centered ca. 0.9 (m, 3 H, terminal methyl), 1.30 (s, 30 H, methylene chain), δ centered ca. 2.3 (distorted t with $J \approx 7$ Hz, 2 H, α-methylene), 3.65 (sharp s, 3 H, methoxy). No carboxyl group proton

(41) Bauer, N.; Lewin, S. Z. "Techniques of Chemistry" in "Physical Methods of Chemistry", Part IV; Weissberger A., Rossiter, W. B., Eds.; Wiley-Interscience: New York, 1972; Vol. I, p 84.

(42) Raban, M.; Mislow, K. *Top. Stereochem.* **1967**, *2*, 199.

(43) For discussion of unique aspects of the ^{1}H NMR spectra of fatty acid derivatives see: Crutchfield, M. M.; Irani, R. R.; Yoder, J. T. *J. Am. Oil Chem. Soc.* **1964**, *41*, 129. Hopkins, C. Y.; Bernstein, H. J. *Can. J. Chem.* **1959**, *37*, 775. Inoue, H.; Nakagawa, F. *J. Phys. Chem.* **1966**, *70*, 1108. Ulmius, J.; Wennerstrom, H. *J. Magn. Reson.* **1977**, *28*, 309.

(44) Guy, J. B.; Smith, J. C. *J. Chem. Soc.* **1939**, 615. See also: Timmermans, J. "Physico-Chemical Constants of Pure Organic Compounds"; Elsevier: New York, 1950; p 402.

(45) Killheffer, J. V.; Jungermann, E. *J. Am. Oil Chem. Soc.* **1960**, *37*, 456.

(46) Scott, H. L. *J. Chem. Phys.* **1975**, *62*, 1347.

(47) Wilson, R. H.; Doty, V. E.; Rencz, K. H.; Schram, A. C. *J. Lab. Clin. Med.* **1966**, *67*, 87.

(48) Hawke, J. C.; Hansen, R. P.; Shorland, F. B. *J. Chromatogr.* **1959**, *2*, 547. James, A. T.; Martin, A. J. P. *Biochem. J.* **1956**, *63*, 144.

(49) Whitby, G. S. *J. Chem. Soc.* **1926**, 1458.

absorption from the precursor stearic acid was observed upon scanning downfield at increased sensitivity. The methyl stearate produced in this manner was employed directly in the subsequent aminolysis reactions in view of its demonstrated purity and the harsh conditions of the aminolysis procedure.

Anal. Calcd for $C_{19}H_{38}O_2$: C, 76.45; H, 12.83; O, 10.72. Found: C, 76.58; H, 12.89.

Amines. Immediately preceding use, the phenethylamine and (α-methylbenzyl)amine samples were distilled (two to four times depending on initial purity) under a reduced pressure of purified nitrogen through a steam-heated West-type column packed with 15–20 cm of hollow glass beads. Rejection of the first and last 10–15% volumes per distillation afforded 30–50% of the original amines as clear, colorless liquids. The ^{1}H NMR spectra (20%, $CDCl_3$, 60 MHz) of racemic, (*S*)-(−)-, and (*R*)-(+)-(α-methylbenzyl)amine were identical, provided they were protected from the atmosphere.

Analysis of the amines was accomplished through GLPC using a 12 ft by $^1/_8$ in. stainless steel column (170 °C, 24 mL/min) packed with 20% DEGS on Chromosorb WAW (80/100 mesh). The freshly distilled amines exhibited GLPC purities exceeding 99.9 area %. Optical purities were calculated by using data[50,51] provided by Gottarelli and co-workers. See ref[52] for an extensive and critical discussion of the maximum specific rotation and absolute configuration of (α-methylbenzyl)amine.

a. (*S*)-(−)-(α-Methylbenzyl)amine: from Aldrich Chemical Co., Inc. (puriss., catalog no. 11,556-8); bp 50 °C (6mmHg); $d^{24.2} = 0.949 \pm 0.002$ g/cm^3; $\alpha^{24.2}_D = -35.91 \pm 0.07°$ and $[\alpha]^{24.2}_D = -37.8 \pm 0.1°$ (neat); $\alpha^{26.0}_D = -0.552 \pm 0.002°$ and $[\alpha]^{26.0}_D = -27.3 \pm 0.1°$ (*c* 2.021 ± 0.004, MeOH); optical purity, $p = 96 \pm 2\%$.

b. (*R*)-(+)-(α-Methylbenzyl)amine: from Aldrich Chemical Co., Inc. (Gold Label, catalog no. 11,554-1); bp 42 °C (4mmHg); $d^{24.5} = 0.947 \pm 0.001$ g/cm^3; $\alpha^{24.5}_D = +37.43 \pm 0.08°$ and $[\alpha]^{24.5}_D = +39.5 \pm 0.1°$ (neat); $\alpha^{26.0}_D = +0.563 \pm 0.002°$ and $[\alpha]^{26.0}_D = +27.8 \pm 0.1°$ (*c* 2.028 ± 0.002, MeOH); optical purity, $p = 98 \pm 2\%$.

c. (±)-(α-Methylbenzyl)amine: from Aldrich Chemical Co., Inc. (catalog no. M3, 110-4); bp 53 °C (7mmHg); $d^{24.4} = 0.946 \pm 0.001$ g/cm^3.

d. Phenethylamine: from Matheson, Coleman, and Bell (catalog no. PX0485); bp 67 °C (7mmHg); $d^{24.8} = 0.956 \pm 0.001$ g/cm^3.

Stearamides. Racemic and optically active *N*-(α-methylbenzyl)-stearamide and achiral *N*-phenethylstearamide were prepared through aminolysis of methyl stearate with boric acid as catalyst.[53] The absolute configurations of (*S*)-(−)- and (*R*)-(+)-*N*-(α-methylbenzyl)stearamide were established from the known configurations of the precursor amines[54,55] and are consistent with data reported for the lower homologues of this series.[56]

Numerous repetitions of the following general procedure afforded crude yields of 70–90%, which were unaffected by reaction scale (3–30 g) or an excess of boric acid catalyst (up to 2 mol/mol of starting ester). A mixture of 1 mol of boric acid and 2 mol of the amine per 1 mol of methyl stearate was placed in a one-necked boiling flask equipped with a short-path still head and immersed in a sand-filled heating mantle. The reactive vessel was purged thoroughly with purified nitrogen and then heated at 190–200 °C for 24 h with magnetic stirring as the methanol byproduct and excess amine slowly distilled. When the mixture was cooled to room temperature, the solid product was dissolved in a 3:2 petroleum ether/chloroform mixture, 1 L of solvent per 10–15 g theoretical yield of stearamide product being required. The organic phase was extracted successivly against 5% aqueous HCl, against 5% aqueous NaOH, and finally against triply distilled water and then was filtered and dried over anhydrous sodium sulfate. After the solvent was removed through rotary evaporation under reduced pressure, the crude product was recrystallized from 95% ethanol to constant melting point and specific rotation.

The ^{1}H NMR spectra (5.26 ± 0.05% $CDCl_3$ at 250 MHz) of racemic, (*S*)-(−)-, and (*R*)-(+)-*N*-(α-methylbenzyl)stearamide were identical: δ centered 0.89 (distorted t with $J \approx 6.5$ Hz, 3 H, fatty acid terminal methyl), 1.27 (s, 28 H, methylene chain), δ centered 1.48 (d, 3 H, methyl), δ centered 1.63 (m, 2 H, β-methylene), δ centered 2.15 (t with $J \approx 7.6$ Hz, 2 H, α-methylene), δ centered 5.15 (pentet, 1 H, methine), δ centered 5.78 (br d, 1 H, amido), 7.31 (m, 5 H, phenyl). First-order approximation of the AMX_3 coupling from the methyl and amido doublets affords $J_{AM} = 7.0 \pm 0.2$ Hz and $J_{MX} = 7.2 \pm 0.2$ Hz. The ^{1}H NMR spectrum (5.27 ± 0.05%, $CDCl_3$ at 250 MHz) of *N*-phenethylstearamide exhibited the following absorptions: δ centered 0.88 (distorted t with $J \approx 5.9$ Hz, 3 H, fatty acid terminal methyl), 1.24 (s, 28 H, methylene chain), δ centered 1.56 (m, 2 H, β-methylene), δ centered 2.10 (t with $J \approx 7.5$ Hz, 2 H, α-methylene), ca. 2.8 and 3.5 (A_2B_2 system with midpoint δ 3.2, 2 H each m, phenethyl methylenes), 5.49 (br s, 1 H, amido), ca. 7.2 (m, 5 H, phenyl). The lack of multiplicity in the amido absorption and the mirror symmetry of the A_2B_2 system both suggest that for unknown reasons the amido proton is not spin coupled with the protons of the adjacent methylene. This is in sharp contrast to the spectra of the *N*-(α-methylbenzyl)stearamides, where such coupling affords a nearly first-order AMX_3 system.

a. (*S*)-(−)-*N*-(α-Methylbenzyl)stearamide. From 4.62 g (15.5 mmol) of methyl stearate was obtained 4.11 g (68%) of crude product, which was recrystallized five times to afford 1.5 g (25%) of fine, white needles having a melting point of 88.5–88.7 °C (corrected): $\alpha^{25.0}_D = -0.627 \pm 0.002°$, $[\alpha]^{25.0}_D = -54.0 \pm 0.2°$ (*c* 1.162 ± 0.002, $CHCl_3$).

Anal. Calcd for $C_{26}H_{45}NO$: C, 80.56; H, 11.70; N, 3.61; O, 4.13. Found: C, 80.69; H, 11.68; N, 3.50.

b. (*R*)-(+)-*N*-(α-Methylbenzyl)stearamide. From 3.14 g (10.5 mmol) of methyl stearate was obtained 3.10 g (76%) of crude product, which was recrystallized four times to afford 1.41 g (35%) of fine, white needles having a melting point of 88.5–88.7 °C (corrected): $\alpha^{25.0}_D = +0.631 \pm 0.002°$, $[\alpha]^{25.0}_D = +54.3 \pm 0.2°$ (*c* 1.162 ± 0.002, $CHCl_3$).

Anal. Calcd for $C_{26}H_{45}NO$: C, 80.56; H, 11.70; N, 3.61; O, 4.13. Found: C, 80.46; H, 11.83; N, 3.58.

c. (±)-*N*-(α-Methylbenzyl)stearamide. From 2.83 g (9.48 mmol) of methyl stearate was obtained 2.95 g (80%) of crude product, which was recrystallized four times to afford 0.53 g (14%) of a white powder having a melting point of 74–78 °C (corrected).

Anal. Calcd for $C_{26}H_{45}NO$: C, 80.56; H, 11.70; N, 3.61; O, 4.13. Found: C, 80.66; H, 12.00; N, 3.52.

The melting range of the racemic stearamide, unlike that of the optically pure substance, includes a sequence of phase transitions. The lower temperature is associated with extensive sintering, and the upper temperature appears to be a cloud point. Thus, melting behavior of the amorphous powder is complex, and ordinary interpretations of impurity should not be applied to the 4° range (see Results).

d. *N*-Phenethylstearamide. From 2.83 g (9.48 mmol) of methyl stearate was obtained 3.16 g (86%) of crude product, which was recrystallized five times to afford 1.60 g (44%) of fine, white platelets having a melting point of 90.8–91.4 °C (corrected) (lit.[56] mp 91.8 °C).

Anal. Calcd for $C_{26}H_{45}NO$: C, 80.56; H, 11.70; N, 3.61; O, 4.13. Found: C, 80.50; H, 11.78; N, 3.52.

e. (±)-*N*-(α-Methylbenzyl)butyramide was prepared by reaction of the carefully purified amine with butyryl chloride in ether,[56,57] extraction with 3 N HCl, water, and 5% aqueous KOH, and washing with water until neutral. After treatment with activated carbon and chromatography in silica gel, the solution showed one TLC spot on a silica plate. After removal of solvent by short-path distillation (162–164 °C, (0.6 mm)), it gave white needle-like crystals, mp 32.8–35.4 °C. Since this compound gives poor melting behavior[56,57] its authenticity and purity were confirmed by ^{1}H NMR, ^{13}C NMR, and IR spectra.

Anal. Calcd for $C_{12}H_{17}NO$: C, 75.39; H, 8.90; N, 7.33; O, 8.38. Found: C, 75.53; H, 8.86; N, 7.49.

Spreading Solution. A typical monolayer of the amide surfactant has a total mass of about 3×10^{-5} g and is spread from a solution in highly purified hexane of $(5.259 \pm 0.003) \times 10^{-4}$ M average concentration. In order to prevent an enormous waste of laboriously purified surfactants and solvent, without sacrificing the accuracy of solution preparation, we prepared rather small volumes of 25.02 ± 0.01 cm^3 by weighing 5.101 ± 0.003 mg with a Cahn RG Electrobalance (Class M calibrating weights), equipped with a Hewlett-Packard five digit 3450A digital voltmeter, and diluting at 25 ± 2 °C in a calibrated, acid-cleaned volumetric flask. Amounts of 0.1300–0.1600 mL (±0.0002 mL) were spread on the aqueous subphase with Burroughs-Wellcome Co. Agla micrometer syringes, the area available for spreading being roughly twice that of the close-packed monolayer. Special care was taken to keep the syringe and spreading solution in thermal equilibrium. Spreading solutions were stored in a desiccator containing hexane to minimize evaporation of the solvent during film-balance experiments.

The purification of the hexane spreading solvent required care since the purity of a monomolecular film can be no greater than that of the

(50) Angeloni, A. S.; Cagna, D.; Gottarelli, G. *Ric. Sci.* **1969**, *39*, 35.
(51) Gottarelli, G.; Samori, B. *J. Chem. Soc. B* **1971**, 2418.
(52) Doctoral thesis of M. V. Stewart, University of Georgia, 1979.
(53) Sumimoto Chemical Company, Ltd., British Patent, 1 206 126, 1970; *Chem. Abstr.* **1971**, *75*, 118128. See also *Chem. Abstr.* **1971**, *75*, 133020, 140512s, 140513t, **1974**, *80*, 70423.
(54) Mills, J. A.; Klyne, W. *Prog. Stereochem.* **1954**, *1*, 186.
(55) Pedone, C.; Benedetti, E. *J. Organomet. Chem.* **1971**, *29*, 443. Benedetti, E.; Corrandini, P.; Pedone, C. *Ibid.* **1969**, *18*, 203. Bush, M. A.; Dullforce, T. A.; Sim, G. A. *J. Chem. Soc., Chem. Commun.* **1969**, 1491.
(56) Bezruchko, V. T.; Gracheva, V. M.; Dem'yanovich, V.; Potapov, M.; Terent'ev, A. P. *J. Gen. Chem. USSR (Engl. Transl.)* **1967**, *37*, 1391. See also: Potapov, V. M. *Tetrahedron* **1967**, *23*, 4357.
(57) Vaughan, W. R.; Carlson, R. D. *J. Am. Chem. Soc.* **1962**, *84*, 769.

solvent which delivers it.[22] Furthermore, impurities of high surface activity can be generated by air oxidation of alkane solvents during improper storage.[58] Rigorous application of the following procedure consistently afforded hexane suitable for quantitative film-balance work.

ACS reagent grade hexane (J. T. Baker Chemical Co., mixture of iosmeric hexanes, catalog no. 5–9309) was purified through chemical treatment,[59,60] distillation, and chromatography.[61,62] Four lots of 1.2 L were extracted four times against 120-mL portions of concentrated sulfuric acid and then stirred magnetically overnight with a nitrating mixture consisting of 343 mL of concentrated sulfuric acid, 192 mL of concentrated nitric acid, and 185 mL of triply distilled water. The organic phase of each lot was separated and extracted three times against 120-mL portions of water and twice against the same amount of concentrated sulfuric acid and then stirred magnetically overnight over 360 mL of concentrated sulfuric acid (which remained colorless). Each organic phase was extracted successively against 120 mL of water, three times against 120-mL portions of 10% aqueous sodium carbonate, and four times against water (until neutral to litmus). After being dried over anhydrous sodium sulfate overnight, the four portions of purified hexane were combined and distilled under purified nitrogen from activated (300 °C for 24 h under nitrogen flow) 4A Linde molecular sieves through a 20-cm Vigreux column and spray trap at a rate of 2 ± 1 mL/min, discarding the first and the last ca. 10% volumes.

The distillate was stored over activated 4A molecular sieves in a specially constructed still under purified nitrogen. Immediately preceding use, the hexane solvent was distilled into a pressure-equalizing chromatography column (25-cm length, 5.5-cm diameter, fitted with a coarse sintered-glass frit) attached to the still by a standard-taper joint. The lower half of the column was packed with a slurry of aluminum oxide (Woelm basic, activity grade I) and the upper half with silica gel (60–200 mesh). The takeoff stopcock was fitted with a standard-taper joint to which a receiving flask was attached. Thus, the hexane could be distilled freshly, chromatographed, and collected in a single operation under an unbroken atmosphere of purified nitrogen.

The purity of the hexane solvent was monitored[61] at various stages of the above procedure by recording the ultraviolet absorption spectrum against triply distilled water. The end-absorbance curve of the highly purified hexane was smooth throughout, having no extraneous maxima, and routinely possessed and absorbance of less than 0.5 at 195 nm with the unpurged spectrometer. For comparison, the starting ACS reagent grade hexane consistently exhibited absorbances of 0.5 at 219 nm and 1.0 at 217 nm (the so-called UV cutoff) and was completely opaque at 195 nm. Significant maxima and broad absorption also dominated the 240–310-nm region of the spectrum obtained from the unpurified solvent.

Aqueous Subphase Solutions. Concentrated sulfuric acid of ACS reagent grade was further purified[63] by distilling 2–4-L batches through a 20-cm Vigreux column at a rate of 2 ± 1 mL/min at atmospheric pressure and excluding the first and last 20% volumes from the collected middle cut. Sulfuric acid, rather than grease, was used to lubricate the joints of the all-Pyrex distillation system. Individual analyses[64] of separate batches averaged 97.4 ± 0.3 wt % H_2SO_4 by titration. Aqueous subphase solutions were prepared within ±0.2–0.3% of the stated normality by diluting a known weight (±0.1 g) of the distilled and recently analyzed acid to 1 L in base/acid-washed, uncalibrated Class A volumetric flasks (±0.3 mL).

The water used in chemical preparations and in film-balance work was triply distilled, stored, and dispensed from a self-contained all-glass system as a continuous operation under purified nitrogen. The feed water (Pittsburgh tap) was passed through a Cuno Micro Klean 5-μm filter, a Gelman activated carbon capsule, and a Gelman pleated membrane 3-μm filter to a Corning Mega-Pure still. The distillate from this was collected directly and distilled from an alkaline permanganate stage followed by distillation from a dilute sulfuric acid stage before final collection. The creeping of surfactant impurities along the wet glass surfaces between the second and third stages and also between the storage vessel and the nitrogen vent was prevented by maintaining two hot dry sections by wrapping the tubing with heating tape. Continuous operation of the still afforded high-quality air-equilibrated water having a pH of 5.8 ± 0.1 (23 °C), a specific conductance of (0.8 ± 0.1) × 10^{-6} Ω^{-1} cm^{-1} (25 °C), and optical transparency down to 195 nm in an unpurged UV spectrometer. A weekly control chart was maintained on these properties of the water. Static surface tension measurements reported here used the same apparatus except that the feed water (Durham) was prepurified through a Millipore-RO4 reverse osmosis unit followed by "polishing" through a Milli-O ion exchange unit before entering the distillation system. This produced feed water of higher quality with considerably less effort.

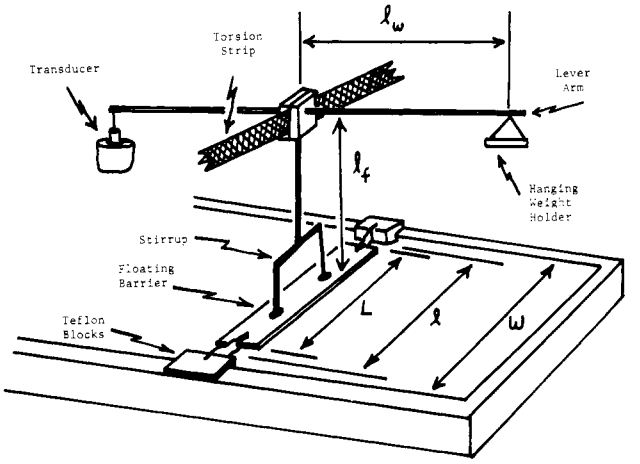

Figure 1. Schematic of torsion head assembly of film balance.

Instrumental Methods. a. Tensiometry. A Fisher Model 215 Autotensiomat surface tension analyzer was used with a Gould 105 strip chart recorder. It was calibrated prior to each individual set of measurements with a Class S weight of 1000.236 ± 0.0185 mg. The performance of the instrument was checked initially by measuring the surface tension of triply distilled water with a ring extraction rate of 0.1 in./min as was used for all measurements. The value obtained at 25 °C was 71.97 ± 0.65 dyn/cm with corrections applied after Harkins and Jordan.[66] This lies easily within experimental error of the value (72.14) tabulated by Adamson.[25]

The surface tension measurements were performed in Teflon dishes, which were cleaned according to the glassware cleaning routine described previously. The surface area available for spreading was calculated from the inside diameter of the rims of the Teflon dishes measured to the nearest 0.01 cm. The diameters averaged 6.69 ± 0.03 cm. The platinum–iridium ring used (Fisher Scientific Co., mean circumference 5.980 cm) was brought to white heat in the oxidizing portion of a gas flame for approximately 1 min before each surface tension measurement. The films were spread from solution in purified hexane, and they were removed by aspiration and overflowing the subphase solution. All experiments were performed in the controlled atmosphere of a Puffer-Hubbard Uni-Therm temperature control unit at 15, 25, and 35 °C.

The enantiomers were used in alternating sequence on the several subphases e.g., the (*R*)-(+)-amide on 3 N H_2SO_4, the (*S*)-(−)-amide on 4 N H_2SO_4, the (*R*)-(+)-amide on 6 N H_2SO_4, and so on, to 14N H_2SO_4.

Film-Balance Equipment. The film balance was designed (by B.K.) so that only Teflon parts would contact the subphase and spread film. The rectangular trough, 14 × 80 × 0.5 cm, was milled from Teflon and bolted permanently inside a magnesium base. Sweeping barriers were also made of Teflon through which stainless steel rods were inserted to prevent warping. One barrier is driven by a worm-screw assembly that is mounted beneath an aluminum base. The sealed reversible motor (ElectroCraft Corp., Model E-550) and precision feedback controller maintain constant speeds and torques from 0 to 50 rpm when connected through a clutch. Double-dial settings and a panel meter indicate speed reproducibly. The trough has a well for Blodgett dipping and a drain for removing the subphase.

A torsion head assembly (Figure 1) employs an FEP-type Teflon float and end barriers. A braced aluminum frame supports it. The two arms

(58) Pomerantz, P.; Clinton, C. W.; Zisman, W. A. *J. Colloid Interfac. Sci.* **1967**, *24*, 16. Doyle, W. P.; Ellison, A. H. *Adv. Chem. Ser.* **1963**, *No. 43*, 268.
(59) Tongber, C. O.; Jonstong, F. *Ind. Eng. Chem.* **1963**, *25*, 733.
(60) Fuchs, L. *Spectrochim. Acta* **1942**, *2*, 243. Castille, A.; Henri, V. *Bull. Soc. Chem. Biol.* **1924**, *6*, 299.
(61) Maclean, M. E.; Jencks, P. J.; Acree, S. F. *J. Res. Natl. Bur. Stand.* **1945**, *34*, 271.
(62) Pertemer, M. *Angew. Chem.* **1951**, *63*, 118. Heese, G.; Schildknecht, H. *Ibid.* **1955**, *67*, 737. Potts, W. J. *J. Chem. Phys.* **1952**, *20*, 809. Mair, B. J. *J. Res. Natl. Bur. Stand.* **1945**, *34*, 435.
(63) Kunzler, J. E. *Anal. Chem.* **1953**, *25*, 93.
(64) Vogel, A. I. "A Textbook of Quantitative Inorganic Analysis", 3rd ed.; Wiley: New York, 1961. Kolthoff, I. M.; Sandell, E. B. "Textbook of Quantitative Inorganic Analysis", 3rd ed.; The MacMillan Co.: New York, 1952; Chapter 2.
(65) Complete redetermination of the dimensions of the apparatus after 1 and 2 years of use showed no significant change within the estimated standard deviation.
(66) Liler, M. "Reaction Mechanisms in Sulfuric Acid"; Academic Press: New York, 1971.

of the U-shaped stirrup, which is connected to a phosphorus-bronze torsion strip, are inserted loosely through the floating barrier with sliding Teflon sleeves. A small cross-arm inverted T balance transforms movement of the Langmuir float detector to the core of an LVDT (i.e., linearly variable differential transducer). The transducer coil (Schaevitz TR-100 and 100MS-L) has a voltage output which is a linear function of the core position and a maximum sensitivity of 0.001-in. movement full scale. For most routine work, however, a sensitivity of 0.01-in. full scale is generally employed. Calibration is achieved by the addition of small weights that deflect the cross arm by known force. The torsion head can stand alone and is removed easily to facilitate acid cleaning of the Teflon trough.

Surface potentials were measured by the ionizing electrode method. A small radioactive source is mounted on the end of a brass electrode. A silver wire is used for the ground connection to a Keithley 616 digital electrometer. The insulated ionizing electrode holder has a rack and pinion adjuster for accurate placement above the surface. It is bearing-mounted to permit scanning of the entire length of the trough (to check for patchy films) and can be swung out of the way without dismounting when not in use. A Sargent two-pen recorder displays the electrometer and LVDT output.

Temperature control of the subphase was achieved, for most of the work reported here, by a serpentine glass cooling coil through which water from a thermoregulator is circulated. It runs the length of the trough and can be removed for acid cleaning. The temperature of the subphase and the air within the Plexiglass case, in which the film balance is housed, can be monitored with Yellow Springs Instrument Co. probes. The probes are connected to a Model TUC Tele-Thermometer, which has a reported sensitivity of ±0.15 °C.

The entire system, including the film balance case, is housed in a Puffer-Hubbard Uni-Therm-800 thermostated cabinet having a programmed Honeywell temperature control unit with a rated temperature range of (2–102) ± 0.1 °C. The relative humidity in the case housing the film balance is monitored by an Abbeon hygrometer.

Calibration and Standardization of Film-Balance Equipment and Determination of Physical Constants. The most important property of monolayers to be studied is the relation between surface tension (surface pressure) and surface area per molecule. Surface pressure is measured as force in dyn/cm exerted against the floating barrier which divides the surface of the film-balance trough (Figure 1). With our apparatus this measurement is made by using a torsion balance with a sensitive LVDT detector on one arm of the balance and a small basket which can receive calibrating weights on the other arm. The LVDT readout can be calibrated with accuracy in terms of dyn/cm, as described by Gaines,[22] through accurate measurement of l_f, the height of the balance arm above the surface of the liquid, l_w, the length of the balance arm which bears the hanging weight basket, l_{eff}, the effective[22] length of the floating barrier, and g, the acceleration due to gravity at the site of the film balance. Calculation of the molecular area requires knowledge of the amount of surfactant spread as a film and the actual dimensions of the surface which contains it. In principle, the determination of these dimensions involves the most elementary level of physics and geometry. In practice, the calibrations are anything but trivial and were repeated before each run in order to assure that the observed differences, which were to be attributed to a deliberately varied property of the system were not confused with artifacts produced by gradual wear and tear on the apparatus.[65]

Linear measurements were made either with an L.S. Starrett Co. steel rule calibrated in 0.5-mm graduations, a Lufkin steel caliper, engraved, to ±0.001 in. or a Griffin and George no. 7149 cathetometer with vernier calibrated to ±0.001-cm graduations. The latter instrument was especially useful for obtaining l_f, a crucial dimension, which could be estimated only rather crudely otherwise. Furthermore, by using the cathetometer, it was possible to fill the trough precisely to the same depth for each measurement. This was a significant factor in obtaining reproducible force-area data.

Since we were hoping for at least three-figure accuracy, the acceleration due to gravity, which was used for all film-balance calculations reported here, was determined for our Pittsburgh laboratory from the International Latitude Formula with correction for elevation and an additional correction from the regional Bougver anomaly map (US Geological Survey) by Dr. Walter L. Pilant of the Department of Earth and Planetary Sciences, University of Pittsburgh. The value for g is 980.10 ± 0.02 cm/s^2 at 1042.5 ft above sea level at latitude of 40°26.7′ N. In our laboratory at Durham, it is 979.72 cm/s^2.

The torsion head was calibrated in terms of mm of pen displacement on the strip chart recorder per mg of weight introduced into the hanging basket on the torsion arm. This calibration "constant" was redetermined before each film was spread. Class S weights were used, which in turn had been calibrated (±0.015 mg) against more accurate Class M weights using the Cahn RG electrobalance.

Compression rates were measured by using a Precision Scientific Co. *Time-It* clock to time the barrier's travel for distances along a 150-cm L.S. Starrett steel rule that was attached to the side of the magnesium base of the trough. The clock could be read to ±0.1 s and the rule to ±0.5 mm. Typical compression times were 900 s. With the motor speed selector locked at its usual position of 1.86, a rate of 0.040 57 ± 0.000 122 cm s^{-1} was normally used.

Film-Balance Operation. All Teflon and glass parts of the film-balance assembly were cleaned routinely using the rigourous procedures necessary to preclude contamination by film-forming materials. The film balance was moved to a stainless steel fume hood, and the torsion head was removed; then the Teflon trough was filled repeatedly to overflowing with hot concentrated HNO_3/H_2SO_4 while the glass cooling coil was still in place. When the mixture was cooled, the acid was removed by suction and the trough was washed thoroughly with once-distilled water and then scrubbed with 95% ethanol using filter paper as a buffer pad. After several washings in this manner, the trough was rinsed with distilled water and replaced in the Plexiglass casing. It was left filled with distilled water for several hours and then suctioned dry, and filled with the aqueous subphase. The floating barrier and other Teflon parts were immersed in hot acid for several hours, rinsed with and soaked in first-stage distilled water, and stored in the glassware oven until needed. The moving barriers were first placed on a flat, solid surface and polished on all sides with Wet-or-Dry Tri-M-ite silicon carbide emery paper (3M Co). They were then base- and acid-washed, rinsed with water, and stored in the oven also. The heat sensitive Teflon sleeves, which protect the stirrup on the torsion head, were soaked with 95% ethanol, rinsed with water, and patted dry with filter paper. Teflon-coated forceps and tweezers used to assemble the floating-barrier attachments were dipped in hot acid, allowed to soak in 95% ethanol, and rinsed with distilled water when needed. The metal screws which hold the ribbons in place were dipped in molten paraffin to render them nonwettable. Before everything was reassembled and replaced in the Plexiglass case, the housing and aluminum base were swabbed with 95% ethanol.

The surface of the subphase solution was cleaned by sweeping with a succession of Teflon moving barriers and the surface contamination removed by suction. The disposable pipets used for this purpose were all base and acid cleaned and stored in the oven. Sweeping of the surface was continued until no surface pressure was detectable on compression at the most sensitive LVDT setting (0.001-in full scale). When the level of the subphase solution was carefully adjusted to afford the predetermined value of l_f, the torsion head was calibrated. The floating-barrier attachments were adjusted until the distance deflected on the recorder strip chart closely approximated that obtained without the floating barrier in place. After calibration, the accumulated contamination was swept away, the level of the subphase solution in the trough readjusted, and the film spread from a solution of the amide in hexane. This was done by just touching the clean surface with the tip of the needle of the Agla micrometer syringe, held at approximately the same angle (about 45° to the surface) throughout the spreading operation. The syringes were cleaned with 95% ethanol, and the glass parts were also cleaned occasionally in hot acid. They were stored in the perforated glass thimble of a Soxhlet extractor over gently refluxing hexane spreading solvent.

The drops of spreading solution were placed carefully on several different regions of the entire available surface area, confined between the floating barrier and the barrier used for compression. The average volume of solution spread was 0.1474 ± 0.0002 mL on an initial surface area of 565.4 ± 1.0 cm^2 (10^{16} Å^2/cm^2). After the film was spread, 20 min elapsed before compression, so that all of the solvent could evaporate and the molecules could distribute themselves evenly over the surface.

Checks for leakage of the film material beneath the barriers were made frequently by sprinkling roasted talc on the film-covered surface. Removal of the surface film was accomplished by sweeping away from the floating barrier and aspirating the surface as described previously. Sweeping was always performed on both sides of the floating barrier. Petri dishes of water were also kept in the film balance case in an attempt to keep the relative humidity and the temperature of the air reasonably constant.

All procedures were performed while wearing polyethylene disposable gloves (Fisher Scientific Co.). These were shown to be free of surface-active contaminants. The surface laboratory itself was isolated from all chemical preparations. All the windows of the laboratory were sealed, the only other opening in the room being covered with three layers of filters to remove larger dust particles. Microadhesive mats (Cole-Palmer Co.) were placed on the floor just inside the door of the laboratory to reduce the introduction of dirt into the room from the shoes of the experimenters. A dust precipitator ionized and removed dust particles from the air. All surfaces were cleaned routinely with 95% ethanol, and the floor was swept and mopped as needed. Every reasonable effort was

Table I. Melting Properties of Crystals as Determined by Differential Scanning Calorimetry

sample	transition temp, °C	heat of fusion ΔH_{fus}, kcal/mol
(*R*)-(+)-*N*-(α-methylbenzyl)stearamide	89.0	1.82 ± 0.12
(±)-*N*-(α-methylbenzyl)stearamide	73.3, 76.1	1.43 ± 0.08
phenethylstearamide	91.7	1.55 ± 0.08

made to preclude contamination of the spread films with dust or any adventitious film-forming materials.

Differential Scanning Calorimetry. The thermal phase transition temperatures and enthalpies of crystalline samples were studied by using a Perkin-Elmer DSC-1B differential scanning calorimeter in the laboratory of Professor J. H. Magill (Materials Science Department, University of Pittsburgh). Samples of 1.0–3.0 mg were sealed hermetically in volatile sample aluminum pans and were equilibrated thermally in the sample cell under a nitrogen atmosphere until a horizontal base line was obtained; then the heating and cooling thermograms were recorded at rates of 1.25, 2.5, and 10 °C/min against a reference cell containing an empty pan. The instrument was calibrated (±0.05 °C) at each of these rates with a set of Fisher certified thermetric standards (catalog no. T-418) of triple point: *p*-nitrotoluene (51.55 °C), naphthalene (80.24 °C), benzoic acid (122.33 °C), and adipic acid (151.53 °C). Transition temperatures were corrected for the lag in temperature between the sample and the holder. The areas of the heating curves were measured by triangulation and converted to enthalpies of phase transitions. Calibration of these calorigrams was based on the sharp and symmetrical transition peak of the benzoic acid heating curve (Fisher certified primary standard, catalog no. A-68, ΔH_{fus} = 4.134 kcal/mol) which was measured alternately with the experimental samples.

Results

Differences in behavior between pure enantiomers and their racemic modification are commonly observed in crystals. We shall present our results first by comparing the properties of our crystalline stearamides in terms of melting, solubility, and X-ray powder data. We will then consider two kinds of surface energy measurements: surface tension and equilibrium spreading pressure, under static conditions at constant area, but with variation of acidity and temperature. The thermodynamics of spreading will be compared with the distribution behavior of *N*-(α-methylbenzyl)butyramide between hexane and aqueous sulfuric acid as a crude model for film spreading.

With this background we will be able to discuss the force-area curves as a function of acidity, temperature, and film composition in order to characterize the aggregation phenomena in the films and to differentiate thermodynamic from kinetic behavior, which will be discussed in subsequent papers.

Investigation of Crystalline Solids. It was apparent, even in the early stages of purification, that there was a marked difference between the melting behavior of the racemic and optically pure enantiomeric *N*-(α-methylbenzyl)stearamide samples. Also, not surprisingly, the crystals of the structural isomer *N*-phenethylstearamide behaved differently. The racemic crystals, recrystallized four times from 95% ethanol, melted over a range of 4 °C (mp 74–78 °C (corrected)). The enantiomers, on the other hand, had a melting range of only 0.2 °C (mp 88.5–88.7 °C (corrected)). The racemic crystals were about three times as soluble in hexane at 25 °C as were the enantiomers (i.e., 1.01 vs. 0.37 mg/mL), representing a difference of about 0.60 kcal/mol in the free energies of solution. Since the heat of fusion (Table I) of the racemate is also less endothermic by 0.39 kcal/mol, its greater solubility is determined both by enthalpy and entropy factors.

The thermal phase transition temperatures and enthalpies of the crystalline stearamide derivatives were studied by differential scanning calorimetry (DSC). The results of many replica runs are shown in Table I. Sharp differences were observable between the melting and cooling behavior of the enantiomers, their racemic modification, and the structural isomer. The DSC thermogram of the racemate showed several peaks, whereas crystals of the pure enantiomers and those of the achiral structural isomer gave single sharp peaks which persisted despite variation of scanning speed.

The powder diffraction patterns of the racemic and enantiomeric stearamides were obtained, under the direction of Professor Richard Butera (Department of Chemistry, University of Pittsburgh) using a Diano X-ray diffractometer (XRD-700). Plots of intensity vs. angle of rotation show that there is a considerable difference between the angles of the three major peaks for the racemic and enantiomeric stearamides. The differences between the packing in the crystals were further emphasized by differences in the *d* spacings calculated from 10 through 30 *d*. Because of the differences observed between the two diffraction patterns, the racemic modification can be termed a true racemic compound or racemate. This bears out the fact that the intercrystalline forces in the enantiomeric and racemic stearamides are different and are sensitive to changes in the spatial arrangement of the molecules in the solid state.

Stability Studies. All of the measurements of surface properties for the stearamides reported here would be meaningless if these compounds were not chemically stable under the conditions of the experiments. Although the rates of acid-catalyzed amide hydrolyses are usually very slow at room temperature,[66] it should not be assumed that hydrolysis had not occurred during our experiments. Several facts secure the stabilitites of our compounds under the conditions of these studies.

First, it should be recognized that the hydrolysis products from the *N*-(α-methylbenzyl)stearamides or *N*-phenethylstearamide would be stearic acid, whose surface properties have been characterized extensively, and the ammonium salt, which would be dissolved instantly in the aqueous acid subphase. Obviously, none of the differences which we have observed between the surface properties of the chiral and achiral stearamides could possibly have been detected if they had been hydrolyzed after spreading on the acid subphase. In several experiments, films were held at constant pressure for 24–48 h on 10 N acid without loss of film pressure or area. It is reasonable that films handled under all milder conditions were also stable.

A further check was provided by the stability of *N*-(α-methylbenzyl)butyramide, which was prepared for the distribution studies to be described below. This compound, unlike the very hydrophobic stearamides, has an appreciable solubility in aqueous acids with strong UV absorption over the range of 200–270 nm. Samples of this compound were stirred in 10 N aqueous sulfuric acid for 1 week at room temperature with no observable change in the spectrum. Likewise, crystals of the stearamides were stirred with 10 N acid for 5 days at room temperature with no appearance of the spectrum of the corresponding (α-methylbenzyl)ammonium ion in the acid solution.

Finally, we note that Menger and Jerkunica[67] were able to use *N*,*N*-dimethyldodecamide as a surfactant in aqueous sulfuric acid solutions up to 95% without evidence of decomposition.

Static Surface Tension Lowering. Surface tensions were measured by the Du Nouy ring method using a Fisher Scientific Co. Autotensiomat which provides a strip chart record of the force produced on a hanging ring as the surface in a thermostated beaker is lowered by means of a screw driven platform jack supporting the beaker. A point of maximum tension occurs just before the ring detaches from the surface[68] and is more reproducible than the detachment point. The Autotensiomat also has the advantage that it can be operated by remote control and can, therefore, be set up inside a Puffer-Hubbard temperature-controlled cabinet to improve thermostating and reduce surface contamination.

Our previous discovery of acid-dependent chiral discrimination in monolayers of *N*-(α-methylbenzyl)stearamide[19] employed a hand-operated Cenco tensiometer. The results presented in Table II were redetermined by using the Autotensiomat. As shown in Figure 2, more regular trends are seen in the dependence of surface tension lowering than in our previous results, and a more constant difference has been found between the racemic and enantiomeric films. Measurements of surface tension lowering by films of

(67) Menger, F. M.; Jerkunica, J. M. *J. Am. Chem. Soc.* **1979**, *101*, 1896.
(68) Harkins, W. D.; Jordan, H. F. *J. Am. Chem. Soc.* **1930**, *52*, 1751.

Table II. Surface Tension Lowerings by Racemic and Enantiomeric Films of *N*-(α-Methylbenzyl)stearamide on Sulfuric Acid Subphases at Various Acid Strengths and Temperatures[a]

	Δ (±)[b]			Δ (+) or (−)[c]		
acidity, *N*	15 °C	25 °C	35 °C	15 °C	25 °C	35 °C
4	0	0	1.4 ± 0.5	0	0	0
6	1.4 ± 0.3	4.5 ± 0.9	6.0 ± 1.0	0	0	1.8 ± 1.3
8	7.8 ± 0.7	7.1 ± 1.8	12.6 ± 0.6	2.2 ± 0.8	3.5 ± 1.1	7.8 ± 0.3
10	13.3 ± 1.7	11.7 ± 1.5	16.2 ± 1.3	6.4 ± 1.6	7.0 ± 1.2	14.0 ± 0.2
12	17.2 ± 1.3	16.9 ± 1.3	21.9 ± 1.8	8.6 ± 1.2	15.2 ± 1.6	19.7 ± 0.3
14	20.6 ± 1.1	23.7 ± 2.8	23.1 ± 0.5	13.9 ± 2.6	20.1 ± 1.3	26.6 ± 1.0

[a] Measurements in dyn/cm at 60 Å²/molecule refer to difference between the surface tensions of pure acidic subphase and that covered with monolayer of the amide. [b] Surface tension lowering produced by racemic film. [c] Surface tension lowering produced by an enantiomeric film.

Table III. Surface Thermodynamic Properties from Surface Tension Lowering by *N*-(α-Methylbenzyl)stearamide on Aqueous H_2SO_4 Subphases at 25 °C

	$\Delta G°$,[a] kcal/mol		$\Delta S°$,[b] Gibbs/mol		$\Delta H°$,[c] kcal/mol	
acidity, N	racemic	*R*(+) or *S*(−)	racemic	*R*(+) or *S*(−)	racemic	*R*(+) or *S*(−)
4	*d*	*d*			*d*	*d*
6	−0.39	*d*	19.9		5.5	*d*
8	−0.61	−0.30	20.7	24.2	5.6	6.9
10	−1.01	−0.60	12.5	32.8	2.7	9.2
12	−1.46	−1.31	20.3	48.0	4.6	13.0
14	−2.05	−1.74	10.8	54.9	1.7	14.6

[a] $\Delta G° = (\gamma - \gamma_0) \times 60 \times 1.44$, average error is ±0.23 kcal/mol. [b] Calculated from change in surface tension lowering from 15 to 35 °C, average error is ±13 Gibbs/mol. [c] From $\Delta H° = \Delta G° + T\Delta S°$. [d] Less than 0.2 kcal/mol.

racemic and enantiomeric stearamides were made at 15, 25, and 35 °C and are reported in Table II. Each value is the mean of five to nine measurements. The derived surface thermodynamics are presented in Table III.

Equilibrium Spreading Pressures. The equilibrium spreading pressure (ESP) of a monomolecular films is that pressure at which the molecules in the monolayer are in equilibrium with the stable bulk crystalline phase. To measure this property, we placed highly purified crystals of either the enantiomeric or racemic stearamides, or a 1:1 mixture of the two enantiomers, very carefully on the clean aqueous acid surface. The crystals were always in large excess over the amount of material required to cover the surface area used (565 cm²). The subphases used were 6 and 10 N H_2SO_4, and the temperature was kept constant, while the change in film pressure at constant area was noted as a function of time on the strip chart recorder. Attainment of ESP was verified by advancing the barrier a few centimeters to raise the pressure by about 2 dyn/cm and observing that the pressure relaxed to its original value after compression had been stopped or when more crystals were added to a film-covered surface and observing no rise in pressure. Over the 12-h (or longer) period that each individual set of crystals remained on the surface, care was taken to maintain a constant level of the subphase solution in the trough.

Spreading of films from crystals can depend on the state of the crystal, and the ESP should ideally be developed from a monolayer in equilibrium with a single perfect crystal. Our results are somewhat compromised by our inability to grow large single crystals of the racemate. In our hands, this was always formed as a fine powder. However, the values reported here were reproducible for different amounts of crystals grown from different batches and the crystalline character has been demonstrated by its DSC and X-ray powder behavior.

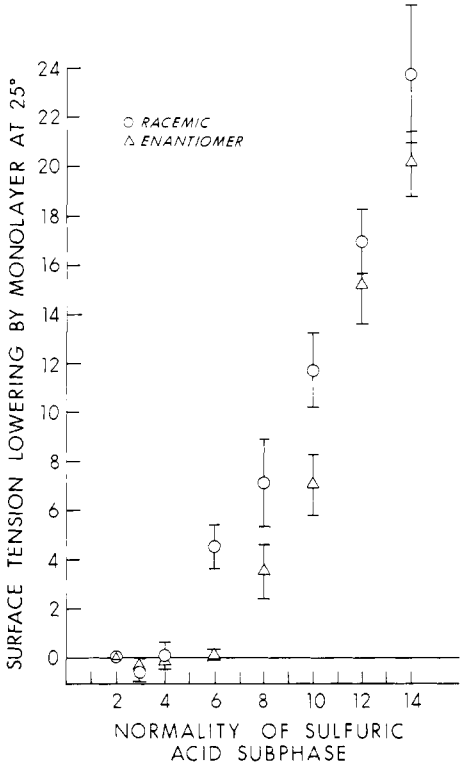

Figure 2. Surface tension lowering of aqueous sulfuric acid solutions by monolayers of *N*-(α-methylbenzyl)stearamide at 25 °C and surface concentration of 60 Å²/molecule.

The racemic stearamide crystals deposited on 10 N H_2SO_4 at 25 °C spread rapidly to form a film whose equilibrium spreading pressure (ESP) of 7.7 dyn cm^{-1} was attained within 5 min (Table IV). On the other hand, spreading of the pure enantiomers was much slower. After 10 min, the surface pressure of the enantiomeric film had begun to build up, but it was not until after 8 h that its ESP of 3.9 dyn/cm was attained.

Table IV. Equilibrium Spreading Pressures (ESP's) of Racemic and Optically Pure *N*-(α-Methylbenzyl)stearamides at Various Temperatures and Subphase Acidities[a]

	10 N H_2SO_4				6 N H_2SO_4			
	racemate		enantiomers		racemate		enantiomers	
temp, °C	π, dyn/cm	*A*, Å²/molecule	π, dyn/cm	*A*, Å²/molecule	π, dyn/cm	*A*, Å²/molecule	π, dyn/cm	*A*, Å²/molecule
15	4.8 ± 0.3	76 ± 3	0.89 ± 0.1	86 ± 3				
25	7.7 ± 0.3	70 ± 3	3.9 ± 0.4	82 ± 3	4.9 ± 0.2	73 ± 1	0.6 ± 0.2	77.5 ± 0.1
35	20.9 ± 0.6		10.3 ± 0.5					

[a] $*A_e$, obtained from normalized π–*A* isotherms, is area at π_e at 15 and 25 °C. Weight of crystals used was about 300 mg. Area of trough = 565.4 cm². π_e is equilibrium spreading pressure (ESP); $*A_e$ is area per molecule at π_e.

Table V. Thermodynamic Properties for Spreading from Crystals for the Chiral Stearamides on 10 and 6 N H_2SO_4[a]

	subphase acidity		10 N H_2SO_4						6 N H_2SO_4	
	$\Delta G_s°$, kcal mol^{-1}		Q_s, kcal mol^{-1}		$\Delta H_s°$, kcal mol^{-1}		$\Delta S_s°$, cal deg^{-1} mol^{-1}		$\Delta G_s°$, kcal mol^{-1}	
temp, K	racemate	enantiomer	racemate	enantiomer	racemate	enantiomer	racemate	enantiomer	racemate	enantiomer
288	−0.525	−0.110	+8.6	+10.7	+8.1	+10.6	28	35		
298	−0.776	−0.461	+8.9	+10.7	+8.1	+10.3			−0.515	−0.066

[a] $\Delta G_s° = -\pi_e A_e$; $Q_s = TA_e d\pi_e/dT$; $\Delta H_s° = Q_s + \Delta G_s°$; $\Delta S_s° = A_e d\pi_e/dT$. See ref 24, p 179 ff.

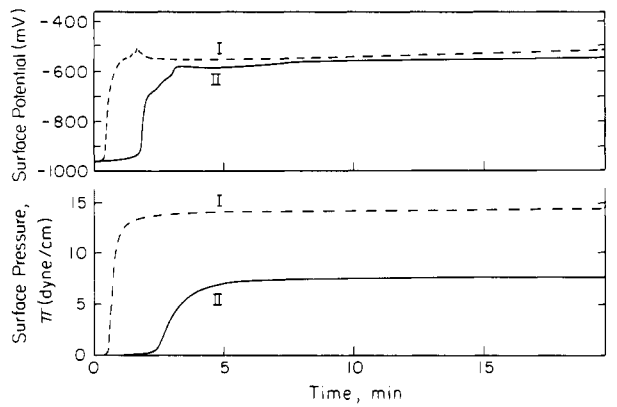

Figure 3. Development of surface pressure and surface potential from crystals of *N*-(α-methylbenzyl)stearamide on 10 N H_2SO_4 at 25 °C. Curve I is for racemate and curve II for pure enantiomers.

When a 1:1 mixture of crystals of the two enantiomers was dusted onto the surface, the final ESP, obtained after 15 h, approximated that of the film spread from racemic crystals. However, the film pressure from the 1:1 mixture was developed slowly compared to that from the racemate, demonstrating the slow release and mixing of enantiomer molecules in the surface.

Figure 3 shows the changes in surface pressure at 25 °C for films from racemic and enantiomeric crystals and also from a 1:1 mixture of *R* and *S* enantiomers. Points refer to surface tension lowerings for the *S* enantiomer measured by tensiometry.

Figure 4 compares changes in surface potential with surface pressure as the ESP is approached on 10 N H_2SO_4 at 35 °C. It is noteworthy that the surface potential is the only surface property for which we have failed to find chiral discrimination for these compounds. ESP values for the racemic and enantiomeric stearamides were also obtained at 15 and 35 °C on 10 N H_2SO_4 and are presented in Table IV.

ESP values for the chiral stearamide were also obtained on 6 N H_2SO_4 at 25 °C. Again, the film spread from a 1:1 mixture of the *R*(+) and *S*(−) crystals came to equilibrium much more slowly than the film spread from crystals of the racemate. After 10 h, the racemate crystals were exerting a pressure of 2.5 ± 0.2 dyn/cm, but it was only after 29 h that the 1:1 mixture attained a pressure of 2.82 ± 0.8 dyn/cm. The racemate's ESP after 17 h was 4.9 ± 0.2 dyne/cm. After 41 h, the 1:1 mixture's ESP was 4.0 ± 0.5 dyn/cm.

The thermodynamic properties for spreading at equilibrium from crystals may be obtained from the temperature dependence of the ESP values. The standard free energy of spreading, $\Delta G_s°$, is evaluated from $\Delta G_s° = -\pi_e A_e$, where π_e is the spreading pressure at equilibrium, ESP, and A_e is the film area per molecule at that pressure. Conversion of dyn cm^{-1} Å^2 molecule^{-1} to cal/mol at a given pressure π is achieved through multiplication of the $-\pi_e A_e$ product by 1.44 cal mol^{-1} cm dyn^{-1} molecule Å^{-2}. The area occupied by the crystals is assumed to be negligible. Since it is not practical to measure the weight of molecules spread from crystals to form the film, the area per molecule at the ESP was read from the force-area curve for films that had been spread from a hexane solution. The heat of spreading, Q_S, may be evaluated from the modified Clausius–Clapeyron equation, where $d\pi_e/dT = Q_S/TA_e$.[24] The enthalpy of spreading, $\Delta H_S°$, is the sum $\Delta H_S° = \Delta G_s° + Q_s$. The entropy of spreading at equilibrium is also dependent on temperature and may be calculated from the relation $\Delta S_s° = A_e d\pi_e/dT$ or simply $\Delta S_s° = Q_s/T$.

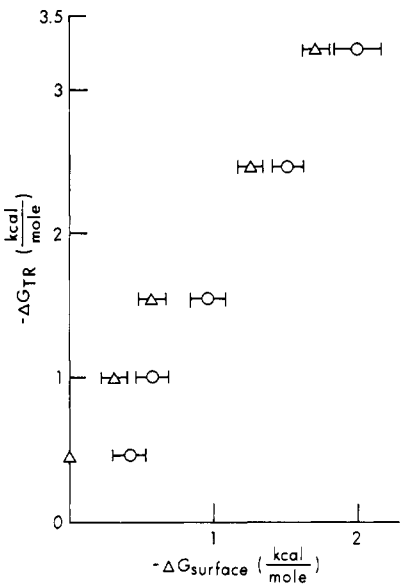

Figure 4. Correlation of free energies of transfer for *N*-(α-methylbenzyl)butyramide from hexane to aqueous acid solutions (Table VI) vs. surface energy reduction by monolayers of (±)- and (*R*)-(+)-*N*-(α-methylbenzyl)stearamides on the same acid solutions (Table III): △, enantiomeric ΔG_γ; ○, racemic ΔG_γ.

The evaluated thermodynamic quantities for the racemic and enantiomeric stearamides are compared in Table V, derived from the listing, in Table IV, of the ESP values obtained at 15, 25, and 35 °C on 10 N H_2SO_4 and at 25 °C on 6 N H_2SO_4. In all cases, $\Delta G_s°$ is small and, of course, negative, since spreading occurs spontaneously. That for the racemate is always more negative and, therefore, shows a more favorable spreading process. Because of the large amounts of heat absorbed on spreading, the enthalpies are all large and positive. Likewise, there is a gain in entropy as the molecules spread from the crystals to the expanded film. The signs and magnitudes are comparable to those calculated by Harkins[24] for spreading of myristic acid on aqueous subphase at pH 2.0.

The ESP values for the chiral stearamides were also obtained by using the Du Nouy tensiometer. Teflon petri dishes of surface area 19 cm^2 were filled to overflowing to ensure a clean surface whose surface tension was measured. After the surface and ring were cleaned again, small crystals were placed carefully on the surface and the surface tension was observed as a function of time. The subphases used were 6 and 10 N H_2SO_4, and measurements were made at hourly and half-hourly intervals. Each timed measurement was made on a different film-covered surface. After several hours at 25 °C the surface tension lowerings on 10 N H_2SO_4 were 3.8 dyn/cm for the enantiomeric stearamide and 5.1 dyn/cm for the racemic.

Liquid–Liquid Distribution Studies. We have observed that the stearamides do not spread to produce monolayer films on water but do spread on aqueous sulfuric acid solutions that are 6 N or stronger where the amides presumably undergo protonation to form an ionized monolayer.[22] As a model to test this behavior, racemic *N*-(α-methylbenzyl)butyramide was prepared, and its

Table VI. Distribution Data for (±)-N-(α-Methylbenzyl)butyramide between Hexane and Aqueous Acid Solutions[g]

acid normality, N	H_A[a]	A_{hex}	A_{ac}	V_{hex}[d]/V_{ac}	D_{obsd}[e]	$-\Delta G_{Tr}°$[f]
H_2O		0.2717	0.5682	1/1	0.4782	0.44
1	0.10	0.2930	0.5522	1/1	0.5306	0.37
2	−0.33	0.3186	0.5260	1/1	0.6057	0.29
3	−0.69	0.3412	0.5079	1/1	0.6718	0.22
4.5	−1.02	0.3002	0.5418	1/1	0.5541	0.35
6	−1.34	0.2717	0.5755	1/1	0.4721	0.44
7	−1.55	0.1982	0.6601	1/1	0.3003	0.69
8	−1.74	0.3800	(0.4840)	4/1	(0.1963)	0.96
9	−1.93	0.2870	(0.5820)	4/1	(0.1233)	1.23
10	−2.08	0.0551	0.8261	1/1	0.6670	1.59
		0.2330	(0.6480)	5/1	(0.0719)	1.55
11	−2.27	0.1980	0.6830	8/1	0.0362	1.96
12	−2.45	0.1060	(0.7770)	8/1	(0.0171)	2.39
13	−2.58	0.1250	(0.7610)	25/1	(0.0066)	2.96
14	−2.77	0.0660	(0.8230)	20/1	(0.0040)	3.26

[a] Reference 73. [b] Optical density of hexane layer at 266 nm. [c] Optical density of acid layer at 266 nm either measured directly or interpolated by difference from loss of A_{hex} after distribution. [d] Volume ratio of layers. [e] $D_{obsd} = (A_{hex}/A_{ac})(V_{ac}/V_{hex})$. [f] Standard free energy of transfer from hexane layer to aqueous acid; $\Delta G_{Tr}° = 1.36 \log D_{obsd}$. [g] Values in parentheses interpolated.

Table VII. Calculation of the pK_{BH^+} of Protonated (±)-N-(α-Methylbenzyl)butyramide by the Solvent Extraction Method[69,70] at 25 °C

normality of H_2SO_4, N	H_A[a]	log D_{obsd}[b]	log $(K'_D - D_{obsd})$[c]	pK_{BH^+}[d]
2	−0.33	−0.218	−1.30	−1.41
4.5	−1.02	−0.256	−1.00	−1.76
6	−1.34	−0.326	−0.72	−1.73
7	−1.55	−0.522	−0.46	−1.49
8	−1.74	−0.707	−0.35	−1.32
				av −1.54 ± 0.20

[a] From reference 73. [b] From Table VI. [c] $K'_D = 0.65$ from a plot of D_{obsd} vs. $h_A D_{obsd}$ (A and W). [d] $pK_{BH^+} = H_A - \log D_{obsd} + \log K'_D - D_{obsd})$.

distribution between hexane and a series of aqueous sulfuric acid solutions was measured.

A stock solution containing 0.836 98 g of the butyramide in 1 L of purified hexane (see Experimental Section) was prepared. Its absorbance, at the maximum near 266 nm, was 0.841. Appropriate volumes of the stock solution and aqueous sulfuric acid were pipetted into 250-mL separatory funnels and shaken for 2 min and then allowed to separate. UV analysis of the layers used Beer's law plots. Equal volumes of hexane and acid could be used from 1 to 7 N, but at higher acidities, the amide was so soluble in the acidic layer that a higher hexane to acid volume ratio was needed. The concentrations of the amide in both layers could be determined both by the loss from the hexane layer or by direct analysis of both layers. Quadruplicate experiments were done at each acidity. Table VI presents the results of these distribution experiments.

It would be reasonable to assume that the increase in solubility of the amide in the aqueous phase as the acidity increases is the result of amide protonation. However, it is well-known that amides, like other weak bases, may undergo substantial changes in solubility without being protonated because of the effect of hydrogen-bonding on the activity coefficient of the neutral base. The data in Table VI were treated according to the method of Arnett, Wu, Bushick, and Anderson[69,70] (Table VII) to yield an estimate of −1.54 ± 0.2 for the pK_{BH^+} of the conjugate acid of the butyramide which is in the reasonable range to be expected for compounds of this type.

Table VIII. Calculation of pK_{BD^+} of (±)-N-(α-Methylbenzyl)butyramide by Variation of Chemical Shifts (δ) for Indicated Protons as a Function of Acidity

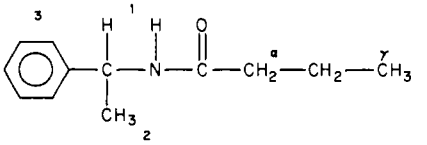

acidity: N of D_2SO_4	$-H_A$[a]	δ_1[b]	δ_α[c]	δ_3	log $(\delta - \delta^B)/(\delta^{BD^+} - \delta)$[d]	pK_{BD^+}[e]
0	−3.03	4.82	2.14	7.28		
1.25	−0.04	4.86	2.20	7.30		
1.65	0.15	4.87	2.22	7.31	−0.73 ± 0.07	−0.88
2.5	0.46	4.91	2.27	7.32	−0.51 ± 0.02	−0.97
3	0.59	4.93	2.30	7.33	−0.38 ± 0.03	−0.97
4	0.83	4.98	2.37	7.35	−0.15 ± 0.02	−0.98
4.62	0.96	5.00	2.38	7.36	−0.10 ± 0.04	−1.06
5	1.03	5.02	2.42	7.37	0.00 ± 0.04	−1.03
6	1.24	5.06	2.47	7.38	0.16 ± 0.06	−1.08
7	1.43	5.09	2.50	7.39	0.30 ± 0.06	−1.13
8	1.61	5.13	2.56	7.41	0.52 ± 0.08	−1.09
9	1.78	5.16	2.59	7.42	0.68 ± 0.08	−1.10
12	2.18	5.21	2.65	7.45		
14	2.55	5.22	2.67	7.45		

[a] Values calculated according to Yates, Stevens, and Katritzky.[73] [b] Representative of averaged chemical shift for the two major peaks of the methine proton indicated. [c] Largest peak of observed triplet for the α methylene protons. [d] Averaged for indicated protons at the particular acidity. [e] Calculated similar to Edward, Leane, and Wang.[78]

pK_{BD^+} of (±)-N-(α-Methylbenzyl)butyramide by ^1H NMR. The protonation of amides in aqueous acids has been examined frequently[71,72] but most extensively by Yates and Katritzky and their co-workers.[73,74] Many amides show sufficient changes in their UV spectra upon protonation to permit determination of the pK_{BH^+} by standard Hammett indicator methods.[71] However, the UV spectrum of N-(α-methylbenzyl)butyramide did not respond sufficiently to acidity change between 1 and 14 N to allow resolution of the effects of protonation from other medium shifts.

An attempt was made to use ^{13}C NMR,[75,76] but to our surprise, the sample suffered extensive heating during the 1–2-h period while spectra were being collected. Led and Peterson[77] have also noted heating of sulfate solutions due to microwave absorption, but, to our knowledge, this limitation on the use of ^{13}C NMR spectroscopy for the study of protonation equilibria has not been noted previously.

The pK_{BD^+} of the butyramide was determined successfully by examination of the ^1H NMR spectrum[78,79] in a series of D_2SO_4/D_2O solutions. The acidities of these solutions were referred to the D_0 scale using the data of Högfeldt and Bigeleisen[80]

(69) Arnett, E. M.; Wu, C. Y. J. Am. Chem. Soc. 1960, 82, 4999.
(70) Arnett, E. M.; Wu, C. Y.; Bushick, R. D.; Anderson, J. N. J. Am. Chem. Soc. 1962, 84, 1674.
(71) Arnett, E. M. Prog. Phys. Org. Chem. 1963, 1, 223.
(72) Rochester, C. D. "Acidity Functions"; Academic Press: London and New York, 1970.
(73) Yates, K.; Stevens, J. B.; Katritzky, A. R. Can. J. Chem. 1964, 42, 1957. Cox, R. A.; Druet, L. M.; Klausner, A. E.; Modro, T. A.; Wan, P.; Yates, K. Ibid. 1981, 59, 1568.
(74) Katritzky, A. R.; Waring, A. J.; Yates, K. Tetrahedron 1963, 19, 465.
(75) Lee, D. G.; Sadar, M. H. J. Am. Chem. Soc. 1974, 96, 2862.
(76) Wan, P.; Modro, T. A.; Yates, K. Can. J. Chem. 1980, 58, 2423.
(77) Led, J. J.; Peterson, S. B. J. Magn. Reson. 1978, 32, 1.
(78) Edward, J. T.; Leane, J. B.; Wang, I. C. Can. J. Chem. 1962, 40, 1521.
(79) Arnett, E. M.; Scorrano, G. Adv. Phys. Org. Chem. 1976, 13, 92 for several references to this method.

and then converted for application to amides by assuming that an equivalent difference between the H_0 and H_A scales would apply to the use of the D_0 scale for amides.

The chemical shifts of the different protons of N-(α-methylbenzyl)butyramide in the D_2SO_4/D_2O solutions are presented in Table VIII. The data were treated by two methods, both of which gave $pK_{BD^+} = -1.02 \pm 0.13$. Plots of δ for protons vs. H_A gave clean sigmoidal plots from which the point of half protonation could be readily determined. Table VIII presents the alternative treatment using the analytical expression $\log (\delta - \delta_B)/(\delta_{BD^+} - \delta) = pK_{BD^+} - H_D$, where δ refers to the chemical shift of the proton under study in the solution of given acidity, δ_B and δ_{BD^+} are the values for the free base in water and its conjugate acid at the highest acidity of D_2O/D_2SO_4, and H_A is the amide acidity function.[73,74] The method of internal comparison of chemical shifts[78] did not produce satisfactory results.

For a comparison of pK_{BD^+} obtained by ^1H NMR with the pK_{BH^+} from the solvent extraction method, the average difference of 0.5 pK unit found by Högfeldt and Bigeleisen for indicators with pK's in the −1 to −2 range was applied. This yields a $pK_{BH^+} = -1.5 \pm 0.2$ which should include safely the accumulated approximations described above.

Discussion

The aim of this research is to investigate the role of molecular shape on aggregation through the use of chiral surfactants distributed as monolayers at the air–liquid interface. This approach combines the ingenious techniques of monolayer chemistry for relating molecular orientation to intermolecular forces with the powerful methodology of stereochemistry for preventing errors due to artifacts or impurities. Despite the obvious relevance of chiral monolayers to biophysical systems such as membranes, there have been remarkably few previous studies of such systems which could serve as guideposts for entering the field.[21]

Our choice of N-(α-methylbenzyl)stearamide for initiating the study was based on such expedient considerations as the ready availability of both enantiomeric (α-methylbenzyl)amines and the rich background regarding their stereochemical properties. The extensive literature on the surface chemistry of stearic acid and its derivatives was also important.

The experiments reported in this paper concern the effects of changing temperature and subphase acidity on the equilibrium surface properties of (R)-(+)-, (S)-(−), and racemic N-(α-methylbenzyl)stearamides and their achiral structural isomer N-phenethylstearamide. The facts, as reported above in the Results, may be summarized as follows.

a. There is a significant difference between the melting points, DSC transition points, heats of fusion, and solubilities of racemic N-(α-methylbenzyl)stearamide compared to those of the enantiomers. Lattice forces in the racemic modification are weaker by all criteria.

b. The racemic material is indeed a racemic compound rather than a racemic mixture, as shown by X-ray powder diffraction patterns.

c. None of the forms of N-(α-methylbenzyl)stearamide lower the surface tension of pure water to an observable degree and therefore do not appear to spread as a true monolayer on that medium. However, on strong (6–14 N) aqueous sulfuric acid subphases, there is appreciable surface activity, and the surface tension lowering is proportional to the amide acidity function of the acid.

d. Acid-dependent chiral discrimination is observed in the monolayer. The racemic amide begins to reduce the surface tension at a lower acidity by several normality units than are required to elicit surface activity from the enantiomers.

e. Equilibrium spreading pressures (ESP's) as measured from pure crystals also show acid dependent chiral discrimination. Again, the racemate spreads more easily and produces a higher surface pressure (for the film in equilibrium with crystals) than do the enantiomers.

f. Both equilibrium spreading pressure and surface tension lowering are highly sensitive to temperature.

g. Previously reported[19] film balance studies also indicate an acid-dependent chiral discrimination factor in the force-area behavior of the monolayers. Again, the racemic films show higher surface pressures than films cast from the enantiomers.

h. No evidence for amide hydrolysis or other decomposition in the monolayer or in solution could be detected even with the strongest acids.

By all criteria, the forces holding the enantiomer molecules together in the crystal and in the spread film appear to be greater than those in the racemic modification. Thus, at any given acidity or temperature the surface free energy lowering is always greater for the racemate than for the enantiomeric film. It is interesting, but probably only fortuitous, that the same relation between stereochemistry and intermolecular forces applies to the relatively disordered monolayer film as holds in the three-dimensional crystal.

Surface Thermodynamics. It is interesting to compare the thermodynamic properties of the monolayer as determined from surface tension lowering at 60 Å²/molecule (Table III) and from the ESP's (Table V) at several temperatures.

The free energy reduction represented by the surface tension lowerings in Tables II and III corresponds to the difference in surface free energy between the monolayer film at 60 Å²/molecule and that of the clean surface or aqueous acid which is lost by spreading the film. The values derived from the ESP's of Table IV include the fact that the film is in equilibrium with its pure crystals and spreads to a molecular area of 70 Å²/molecule for the racemate and 82 Å²/molecule for the enantiomers on 10 N H_2SO_4 at 25 °C. Comparison of Tables III and V shows what we believe to be surprisingly good general agreement between the two sets of thermodynamic properties at 25 °C on 10 N acid. In both sets of experiments the free energy of spreading is markedly more spontaneous for the racemate than for the enantiomers and the enthalpy of spreading is more endothermic for enantiomers.

Returning to Table III to consider the effect of increasing acidity, it is obvious that spreading begins at a lower acidity for the racemate and then levels off at about 8 N with erratic fluctuations of all three properties probably reflecting combined experimental error. The properties of the enantiomeric films follow the same trend but level off at about 10 N acid. Again the racemate is spread more easily and is more easily disrupted by increasing acidity or increasing temperature than is the more tightly packed enantiomer.

Tables I, III, and IV are especially instructive for comparing the stereospecificity of packing in monolayers with crystals. The chiral discrimination factor in surface free energies of monolayers on 10 N H_2SO_4 at 25 °C is 0.30 kcal/mol (Table III); the corresponding free energy difference for spreading from crystals is 0.31 kcal/mol while the difference in free energy of solution in hexane from the crystals is 0.60 kcal/mol.

The chiral discrimination factor on surface enthalpy, under the same conditions, is 11.1 ± 4 kcal/mol (Table III); the heats of spreading difference (Table V) from the crystals is 2.2 kcal/mol while the difference in heat of fusion is 0.39 kcal/mol.

All of the above differences are in the direction of stronger aggregation of the enantiomeric molecules than of the racemic ones. It is not unusual to see fairly large differences between melting points, solubilities, or heats of fusion between crystalline racemates and enantiomers. However, chiral discrimination in solution is negligible by comparison.[18] The relatively large chiral discrimination factors for the free energies and enthalpies of monolayer films bespeak a relatively high degree of order in this "two-dimensional" condensed phase. This confirms the value of chiral monolayers as an approach to the study of intermolecular stereochemistry.

The Mechanism for Acid-Dependent Monolayer Spreading. The most obvious reason why highly acidic subphases should enhance the spreading of stearamide films is that the amide head group, which is constrained to lie in the surface, is undergoing protonation, presumably at the carbonyl oxygen.[71,72,74] There is considerable

(80) Högfeldt, E.; Bigeleisen, J. *J. Am. Chem. Soc.* **1960**, *82*, 15.

precedent for ionization of head groups causing increased expansion of monolayer films.[22] Since amides are weak organic bases which undergo protonation in the 2–8 N range of acidity, it is reasonable that strongly acidic subphases should enhance film spreading. Thus, we may imagine that a rough model for expansion of the film could be provided by the protonation equilibrium of an appropriate *N*-(α-methylbenzyl)amide. The long hydrophobic chain which makes the stearamide a reasonable film former also disqualifies it for direct protonation studies in aqueous acid because of its low solubility. We, therefore, chose the corresponding butyramide as a reasonable model, there being no reason to suppose that the difference in chain length would have a significant effect on the amide basicity.

Two approaches were used to determine the effect of acid variation on the butyramide. One was the ordinary indicator method[71,72] for following the spectral change in homogeneous solutions. The second applied a two-phase distribution method to relate the transfer of amide from a hexane solution to a series of aqueous acid solutions by liquid–liquid partitioning.[69,70]

Table VI records the distribution data for the racemic butyramide at 25 °C. Since it was at high dilution in both media, there was no reason to consider that chirality could affect the distribution constants. Conversion of the logs of the distribution constants into free energies of transfer gives values whose acid dependence may be compared usefully to the effects of acid variation on the surface tension lowering values as presented in Table II. The two formally unrelated free energy properties are plotted in Figure 4 from which a clear correlation is obvious. Thus, the most reasonable process which both studies should have in common is the protonation of the amide function which in one case leads to expansion of the film and in the other to transfer from hexane to the acidic phase.

The pK_{BH^+} of the Amide. Previous work in this laboratory[69,70] showed that liquid distribution studies of the type employed here can be used to determine the protonation constants for weakly basic compounds such as amides. Accordingly, the data were treated as before and a pK_{BH^+} of -1.54 ± 0.20 was determined as shown in Table VII. This falls in the usual range for protonated amides[71,73,74] and may be compared finally to the value obtained by NMR in Table VIII.

The main point of the above studies is to compare the effect of changing acidity on the spreading of the amide films and on well-authenticated methods for determining pK_a's. Figure 4 shows that there is a rough correlation between these two quite different properties and that the proportionality approaches unit slope in the crucial range from 3 to 8 N where the degree of amide protonation in aqueous sulfuric acid is changing most rapidly. The normality at the half protonation point where $H_A = -1.54$ is approximately 7 N. This carries the interesting implication that if the effect of changing acidity is the chief factor causing the amide monolayer to spread; then the surface pK_a of surfactant stearamide and the effective acidity at the interface correspond rather well to that for the bulk aqueous acid. At higher acidities the effect of increasing acidity appears to wane for the surface phenomenon relative to its effect on the distribution ratio. This is primarily because the distribution ratio is not a direct measure of the ionization ratio but contains another term $(K_D' - D)$ where K_D' represents the graphical best estimate of the distribution ratio of the neutral butyramide between hexane and dilute acid media in which transfer due to protonation is negligible.[69,70] Because of Setchenow salting out of the neutral amide by the acid, the simple distribution ratio between hexane and pure water cannot be used for K_D'. The salting out effect is readily noted in the changing concentrations of amide in the hexane layer in the top four entries under A_{hex} in Table VI. Having obtained an independent value for pK_{BH^+} by ^1H NMR, we used it to check the value of $K_D' = 0.65$ that had been estimated graphically from a plot of D_{obsd} vs. $h_A D_{obsd}$.[69,70] The analytically calculated value was 0.73, in very close agreement. We refrain from interpreting the linear free energy correlation slope in Figure 4 since there is no good precedent for relating the effects of chain length on these two rather complex distribution processes presented there.

Conclusions

There is a clearly defined difference between the thermodynamics of aggregation of racemic vs. the optically pure enantiomers of *N*-(α-methylbenzyl)stearamide both in the three-dimensional crystalline array and in monolayers at the surface of aqueous sulfuric acid solutions. Furthermore, the chiral discrimination factor and the surface thermodynamics of the stearamides are strongly dependent on the acidity of the subphase.

We propose that the racemic stearamide molecules have a lower aggregation energy in the monolayer than do the enantiomeric molecules. If the aggregation forces are opposed by protonation of the amide head group, the racemic film is more easily expanded (i.e., shows a lower surface free energy) at a given acidity. This model has been tested by studying the distribution of *N*-(α-methylbenzyl)butyramide between hexane (as a model for the surface environment of neutral amide molecules in the monolayer) and a series of aqueous sulfuric acid solutions (as models for the ionizing environment of the protonated head group in the monolayer).

Since a direct proportionality is found between the acid dependence of the surface free energy of the stearamide monolayer and the free energy of transfer of the butyramide, we conclude that protonation is responsible for the acid dependence of surface properties. The reason for the chiral discrimination factor in the packing of molecules in the monolayer remains obscure, but it is much larger than would normally be encountered in a three-dimensional liquid phase. For example, the enthalpy of spreading for the enantiomeric film is greater by about 2.4 kcal/mol than that of the racemic film. We conclude that chiral monolayers are a promising field for the study of intermolecular stereochemistry.

Acknowledgment. We are glad to acknowledge the support from the National Institutes of Health through Grant GM-20386, the National Science Foundation through Grant CHE-7622369, and the R. J. Reynolds Industries Fund of Duke University which made this work possible. Jeff Gold, James Myers, Jerry Mangone, and Eric Arnett provided valuable laboratory assistance. Dr. Richard Butera, Dr. J. H. Magill, and Dr. Walter Pilant of the Chemistry, Engineering, and Earth and Planetary Sciences Departments of the University of Pittsburgh and Dr. Tomlinson Fort of Carnegie Mellon University provided invaluable help and advice.

Registry No. (±)-*N*-(α-Methylbenzyl)stearamide, 34524-44-2; (*R*)-*N*-(α-methylbenzyl)stearamide, 34524-45-3; (*S*)-*N*-(α-methylbenzyl)-stearamide, 34524-46-4; (±)-*N*-(α-methylbenzyl)butyramide, 79919-40-7; methyl stearate, 112-61-8; (±)-(α-methylbenzyl)amine, 618-36-0; (*S*)-(α-methylbenzyl)amine, 2627-86-3; (*R*)-(α-methylbenzyl)amine, 3886-69-9.